Pacific Northwest
NATIONAL LABORATORY

PNNL-36641

Thermodynamics of Tritium Trapping by Point Defects in Intermetallic $Al_{12}(TM)_{2.35}$ Aluminide Coating Phase

September 2024

Michel Sassi
David J. Senor
Andrew M. Casella

U.S. DEPARTMENT OF ENERGY | Prepared for the U.S. Department of Energy under Contract DE-AC05-76RL01830

DISCLAIMER

PACIFIC NORTHWEST NATIONAL LABORATORY
operated by
BATTELLE
for the
UNITED STATES DEPARTMENT OF ENERGY
under Contract DE-AC05-76RL01830

Printed in the United States of America

Available to DOE and DOE contractors from
the Office of Scientific and Technical Information,
P.O. Box 62, Oak Ridge, TN 37831-0062
www.osti.gov
ph: (865) 576-8401
fox: (865) 576-5728
email: reports@osti.gov

Available to the public from the National Technical Information Service
5301 Shawnee Rd., Alexandria, VA 22312
ph: (800) 553-NTIS (6847)
or (703) 605-6000
email: info@ntis.gov
Online ordering: http://www.ntis.gov

PNNL-36641

Thermodynamics of Tritium Trapping by Point Defects in Intermetallic $Al_{12}(TM)_{2.35}$ Aluminide Coating Phase

September 2024

Michel Sassi
David J. Senor
Andrew M. Casella

Prepared for
the U.S. Department of Energy
under Contract DE-AC05-76RL01830

Pacific Northwest National Laboratory
Richland, Washington 99354

Summary

Density functional theory simulations have been carried out to investigate the potential for tritium trapping by metal vacancies in intermetallic $Al_{12}(TM)_{2.35}$ phase (TM = Fe, Cr, and Ni) as function of temperature and tritium partial pressure. It was found that tritium could be favorably trapped by Fe and Ni vacancies, and some Al vacancies, but not favorably trapped by Cr vacancies. Due to the presence of partially occupied Al sites in bulk $Al_{12}(TM)_{2.35}$, leading to the approximate number of ~255 Al atoms in the unit cell, 86 sites were found energetically favorable to the creation of an Al vacancy. While adding a tritium atom in an Al vacancy is not energetically favorable, the tritiated defect still has a negative Gibbs free energy because the energy gain for creating an Al vacancy overcome the energy cost of adding the tritium species. Based on the calculated Gibbs free energy, the first tritiation of a metal vacancy, at conditions relevant to in-reactor operations, should be more favorable for some Al vacancies, followed Fe, Ni, then Cr vacancies. By comparing the behavior of tritium in $Al_{12}(TM)_{2.35}$ with previously studied Fe-Al coating phases (i.e., $FeNiAl_5$, Fe_4Al_{13}, and $Fe_2Al_{5.6}$), we found that there is a correlation between interstitial tritium solubility and the potential for vacancy trapping. The current trend suggests that if the insertion of an interstitial tritium cost more than 0.3 eV, then trapping by metal vacancies should be preferred. The combination of the simulations results obtained to date suggests that tritium would be more favorable be trapped in inner-iron aluminide coating phases ($FeNiAl_5$, Fe_4Al_{13}, and $Fe_2Al_{5.6}$) than in outer-iron aluminide coating phase ($Al_{12}(TM)_{2.35}$). In the outer-iron aluminide coating phase, $Al_{12}(TM)_{2.35}$, tritium is only weakly trapped by Fe and Ni vacancies while it is preferentially trapped by Al and Fe vacancies for the inner-iron aluminide coating phases ($FeNiAl_5$, Fe_4Al_{13}, $Fe_2Al_{5.6}$). Altogether, these studies show that tritium interacts differently with the various Fe-Al aluminide phases, they also suggest that tritium trapping and retention could be more efficient if metal defects are present and if the solubility of interstitial tritium in the different phases is low.

1.0 Introduction

In the design of the TPBAR the inner surface of the 316SS structural pressure boundary cladding is coated with an iron aluminide (Fe-Al) matrix to reduce tritium permeation into the surrounding coolant. Although most of the tritium is absorbed by the getter, post-irradiation evaluation (PIE) indicates that a small fraction of tritium is trapped in the aluminide coating.[1] The mechanism of how this trapping occurs and how it may be prevented is not known. The purpose of the investigation described in this report is to assess the relative energy of interstitial and substitutional tritium in metal vacancies (e.g., T_{Fe} or T_{Al} sites) in intermetallic $Al_{12}(TM)_{2.35}$. To evaluate the potential for point defects to trap tritium in $Al_{12}(TM)_{2.35}$ phase, constituting the aluminide coating of TPBAR, *ab initio* calculations based on density functional theory (DFT) were used. In order to give a broader trend about tritium trapping potentials in the aluminide coating, the analysis of interstitial binding energies and tritium substitutions in metal vacancies also incorporate theoretical results obtained previously for other Fe-Al phases.[2]

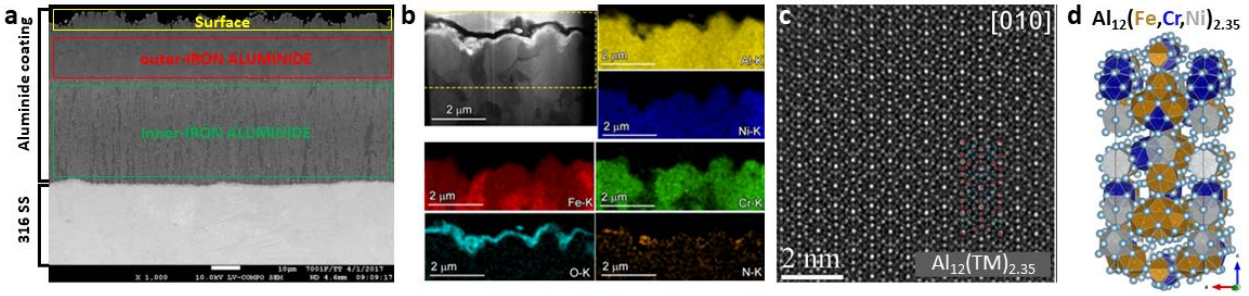

Figure 1: (a) STEM image of the aluminide coating and 316 stainless steel. (b) EDS map of chemical species at surface and near-surface regions. (c) STEM atomic imaging of $Al_{12}(TM)_{2.35}$. (d) Crystal structure of orthorhombic $Al_{12}(TM)_{2.35}$. *STEM/EDS images courtesy of M. Olszta.*[3]

In the STEM imaging of the 316 SS and its aluminide coating, several regions could be identified, as shown in Figure 1a, and were labelled as surface, outer-iron aluminide, and inner-iron aluminide. Previous microscopy analysis performed by Jiang *et al.*[4] and M. Olszta[3] found that a 50 nm thick aluminum oxide (Al_2O_3) layer was formed at the surface of the aluminide coating, as shown by the O K-edge EDS map in Figure 1b. Further STEM investigations[3] revealed that below the oxidized surface, a large near surface region, also labeled as outer-iron aluminide, of about 10 µm thick was contaminated with Cr, Ni, and Fe species as shown by the Cr, Ni, and Fe K-edges EDS maps shown in Figure 1b. The combination of atomic column imaging and associated diffraction analysis indicated that this near surface region is crystalline and that an intermetallic orthorhombic Al-phase containing transition metals (TM) at an approximate composition of $Al_{12}(TM)_{2.35}$ is present in a large portion of the 10 µm near surface region (Figure 1c and 1d). In previous work,[5] we built an atomic model of $Al_{12}(TM)_{2.35}$ (Figure 1d) with a Fe:Cr:Ni ratio matching experimentally determined TM proportions of the examined region (i.e., 59 at.% Fe, 18 at.% Cr, and 23 at.% Ni). While it has been observed that tritium permeation is delayed due to the aluminide coating, the actual mechanisms for tritium trapping are still elusive. So far,

observations show that tritium is trapped “somewhere” in the aluminide coating and not the 316 SS. Because experimental detection of tritium is challenging, we rely on DFT simulations to provide insights into the mechanisms and energetics of tritium trapping in the various Fe-Al phases of the aluminide coating.

2.0 Computational Details

DFT calculations have been performed with the VASP code.[6] All the simulations used the generalized gradient approximation (GGA) exchange-correlation as parametrized in the Perdew, Burke, and Ernzerhof (PBE) functional.[7] A cutoff energy of 350 eV for the plane-wave basis set has been used and spin-polarization has been taken into account. For each simulation, the Brillouin zone was sampled with a Monkhorst-Pack[8] *k*-point mesh of 3×3×2 and the total energy was converged with a criterion of 10^{-5} eV/cell. Due to their similar electronic structure, the pseudopotential of standard hydrogen (^{1}H) has been used to describe tritium (^{3}H), however, to account for the isotopic effect, the mass in the pseudopotential has been modified to matches that of the isotope atom.

Relying on a defect-free atomic model of bulk $Al_{12}(TM)_{2.35}$ previously built,[5] we introduced interstitial tritium and metal vacancy defects for which only the atomic coordinates were allowed to relax. The lattice parameters were kept fixed to their relaxed defect-free bulk structures values. Subsequently, tritium loading of the metal vacancy has been investigated by filling it with several tritium atoms. Multiple configurations were calculated and only the most energetically favorable ones are reported.

To evaluate the relative stability of non-tritiated and tritiated metal vacancies at conditions relevant to in-reactor operation, *ab initio* thermodynamics calculations have been carried out in which the temperature (T) and tritium partial pressure $(p(\mathrm{T_2}))$ dependance of the Gibbs free energy of formation of defects, $\Delta G_f(T, p(\mathrm{T_2}))$, has been calculated using the following equation:

$$\Delta G_f(T, p(\mathrm{T_2})) = (E^T_{\text{defect}} + E^{ZPE}_{\text{defect}} + \Delta\mu(T)_{\text{defect}}) - \left(E^T_{\text{perf}} + E^{ZPE}_{\text{perf}} + \Delta\mu(T)_{\text{perf}}\right) + \sum_i n_i (E^T_i + E^{ZPE}_i + \Delta\mu_i(T, p(\mathrm{T_2}))) \quad (1)$$

where n_i is the number of atoms added/removed of each atomic species i. E^T_i, E^{ZPE}_i, and $\Delta\mu_i(T, p(\mathrm{T_2}))$ are respectively the total DFT energy, the zero-point-energy, and the temperature and T_2 partial pressure dependent chemical potential of each reference species i. In order to account for temperature effect in the various Fe-Al bulk phases, $\Delta\mu(T)_{\text{defect}}$ and $\Delta\mu(T)_{\text{perf}}$ are the temperature-dependent chemical potential of the system with and without defect (i.e., perfect). All the temperature-dependent chemical potentials have been calculated using the following relation:

$$\Delta\mu(T) = (H(T) - H^{\circ}(298.15)) - TS \quad (2)$$

where $H(T)$ and $H^{\circ}(298.15)$ are the system enthalpy at a temperature T and at T=298.15 K, and S is the entropy. Here, $H(T)$, is the Helmholtz free energy as given by $H(T) = -k_B T \ln(Z)$, where Z is the partition function expressed as implemented in the Phonopy code.[9] The calculated temperature dependence of the chemical potential of tritium has been obtained from previous work.[2] The temperature and T_2 partial pressure dependent chemical potential of molecular T_2 has been calculated as:

$$\Delta\mu_{\mathrm{T_2}}(T, p(\mathrm{T_2})) = \mu_{\mathrm{T_2}}(T^{\circ}, p^{\circ}(\mathrm{T_2})) + k_{\mathrm{B}} T \log\left(\frac{p(\mathrm{T_2})}{p^{\circ}(\mathrm{T_2})}\right) \quad (3)$$

where T° and $p^{\circ}(\mathrm{T_2})$ are the temperature and T_2 partial pressure at standard conditions.

3.0 Results and Discussion

3.1 The energy landscape of metal vacancies

In order to investigate tritium trapping by metal vacancies in bulk $Al_{12}(TM)_{2.35}$, a single metal vacancy has been created at each of the 305 atomic sites to identify those most favorable for vacancy formation. For the Al sites, it was found that the creation of a vacancy could lead to a gain of energy in some cases. In particular, 86 sites out of 255 were found to have a negative enthalpy for vacancy generation. To help with the visual localization, these sites are represented by green spheres in Figure 2b and 2c. The sites all happen to be located in band regions of the structure, likely correlated to the position of Al sites with partial occupancy in the experimental structure,[10] shown in Figure 2a. Experimentally, it was determined that the unit cell contains approximatively 305 atoms.[10] This uncertainty plays a role in favor of vacancy creation at the Al sites. In $Al_{12}(TM)_{2.35}$, the defect formation energy of a single Al vacancy ranges from -1.1 eV to 1.6 eV. In order to confirm that the energetically favorable creation of Al vacancy is not correlated to the transition metal mixing, we have generated a single Al vacancy in the iron end-member $Al_{12}(Fe)_{2.35}$ phase and observed a similar distribution of the Al sites having a favorable defect formation energy (Figure 2b). This indicates that the regions favorable for Al vacancy formation is not very sensitive to TM distribution. In the case of $Al_{12}(Fe)_{2.35}$, the defect formation energy of a single Al vacancy ranged from -1.2 eV to 1.4 eV and spanned 93 sites out of 255. In comparison to $Al_{12}(TM)_{2.35}$, this suggests that having a mixing of transition metal in the structure slightly reduces, by about 2.7%, the possibilities for energetically favorable Al vacancy formation.

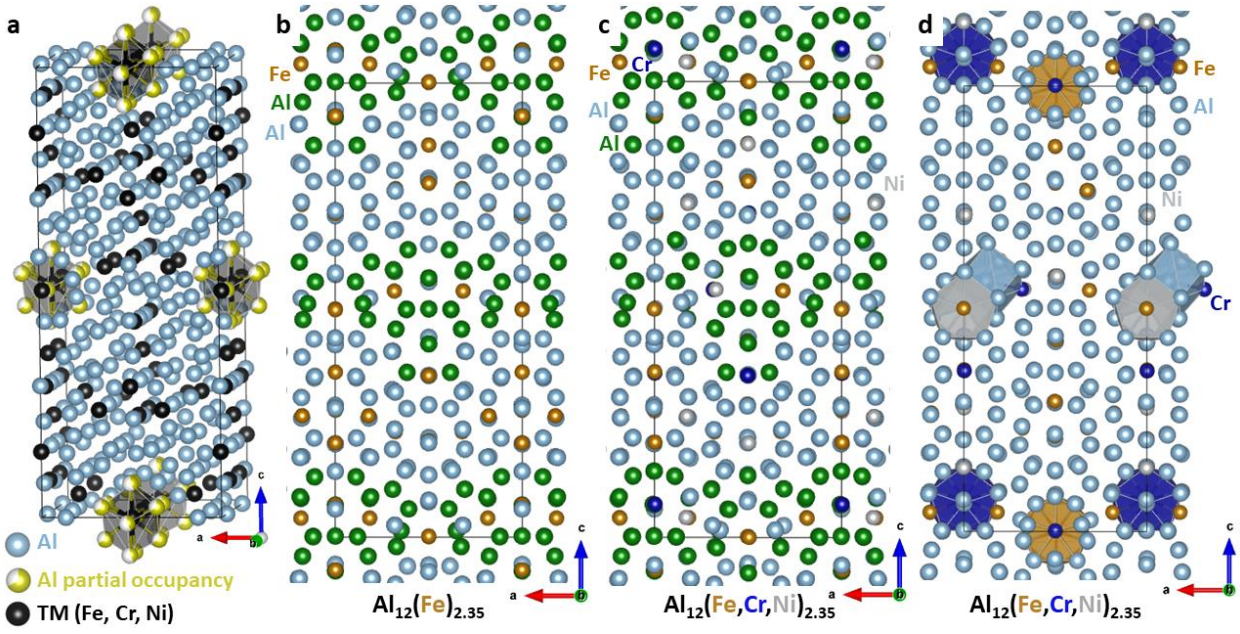

Figure 2: (a) Experimental structure of orthorhombic $Al_{12}(TM)_{2.35}$ with the location of Al partial occupancy sites. (b) and (c) highlight of the "band" regions in which an Al vacancy is energetically favorable to create. The Al sites that allow for a favorable vacancy creation are shown by green

spheres. (d) The polyhedra highlight the location of the most energetically favorable metal vacancies in $Al_{12}(TM)_{2.35}$ for each species.

For Fe, Cr, and Ni species, the vacancy formation energy respectively ranged from 1.1 eV to 2.2 eV, from 1.2 eV to 2.1 eV, and from 1.4 eV to 1.8 eV. To help identify the position of the most favorable sites for vacancy formation, Figure 2d shows a single polyhedron for each species. While vacancy clustering and concentration has not been investigated, we should note that the defect formation energies of vacancies would be affected if other vacancies are generated near each other.

3.2 Temperature dependence and stability of metal vacancies

To evaluate the effect of temperature on the Gibbs free energy of metal vacancy formation, *ab initio* thermodynamic calculations have been performed. The temperature dependance shown in Figure 3 indicates that Fe, Cr, and Ni vacancies are not very sensitive to temperature variations, however, the formation of Al vacancies is found to be increasingly more favorable as the temperature increases.

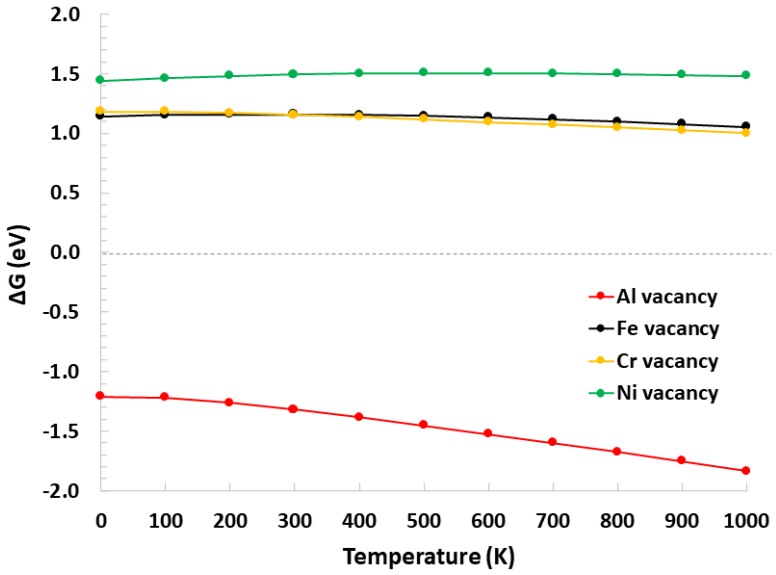

Figure 3: Temperature dependance of the various metal species in $Al_{12}(TM)_{2.35}$.

3.3 Effect of tritium loading and trapping potential of metal vacancies

The tritiation of metal vacancies has been carried out for a loading of up to 5 tritium atoms. As shown in Figure 4, the addition of tritium in metal vacancies generally lead to an increase of

the defect energy. However, the first tritiation of Fe and Ni vacancies only induces a small energy increase of 0.01 eV and 0.07 eV respectively, in contrast, the first tritiation of Al and Cr vacancies induce a larger energy increase of 0.39 eV and 0.59 eV respectively. In the specific case of Al vacancy, up to two tritium atoms can be added before the defect becomes energetically unfavorable. While adding tritium atoms increase the defect energy, it is compensated by the initial energy gain of forming an Al vacancy. As shown in Figure 4, tritium species preferentially form Fe—T, Cr—T, or Ni—T bonds rather than Al—T bonds when trapped into metal vacancies.

To gain insights into the potential for metal vacancies to trap tritium species, it is interesting to compare the energetics between a tritium trapped in a vacancy and an interstitial tritium. In that regard, Figure 4 reports the energy of an interstitial tritium, noted T_i, and a non-interacting T_i and a metal vacancy, generically noted V_M (M= Al, Fe, Cr, or Ni), labeled (V_M+T_i) in the Figure's legend. Al and Cr vacancies do not favorably trap tritium species because the tritiated defect is respectively 0.21 eV and 0.40 eV less energetically favorable than a non-interacting T_i and V_{Al} or V_{Cr} defect. In contrast, Fe and Ni vacancies can favorably trap tritium species because the tritiated defect is respectively -0.18 eV and -0.11 eV more energetically favorable than the non-interacting T_i and V_{Fe} or V_{Ni} defects.

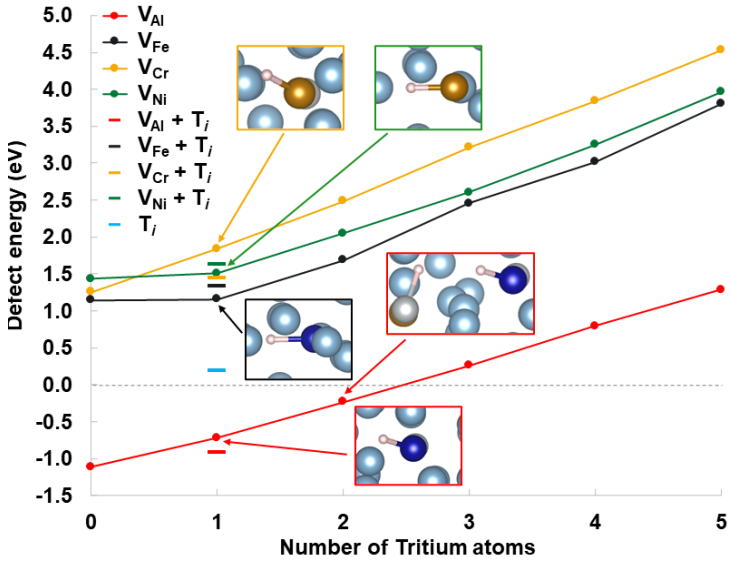

Figure 4: Effect of tritium loading and trapping potential of metal vacancies. The small horizontal lines indicate the energy for a non-interacting interstitial tritium (T_i) and a metal vacancy.

3.4 Effect of temperature and tritium partial pressure

In order to investigate the effect of temperature and tritium partial pressure ($p(T_2)$) on the relative thermodynamic stability of tritiated and non-tritiated metal vacancies, *ab initio* thermodynamic calculations have been performed. This allows calculation of the Gibbs free energy of defects at conditions relevant to in-reactor operation, which are a temperature of ~700 K and tritium partial pressures ranging from 10^{-6} to 10^{2} mbar.[11] Figure 5 summarizes the relative

thermodynamics for the most energetically favorable defects in $Al_{12}(TM)_{2.35}$ phase and the purple area highlights the tritium partial pressure of potential interest.

Interestingly, Figure 5 shows that as the tritium partial pressure increases, tritiated vacancies tend to be more energetically favorable. The singly tritiated Al vacancy becomes a favorable defect ($\Delta G_f < 0$) in the range of tritium partial pressure of interest. The next most favorable defect is an aluminum vacancy with 2 tritium atoms, followed by the singly tritiated Fe vacancy. The less favorable tritiated defects are the Ni and Cr vacancies, with a slight preference for the tritiated Ni vacancy as it is 0.02 eV more energetically favorable than a singly tritiated Cr vacancy.

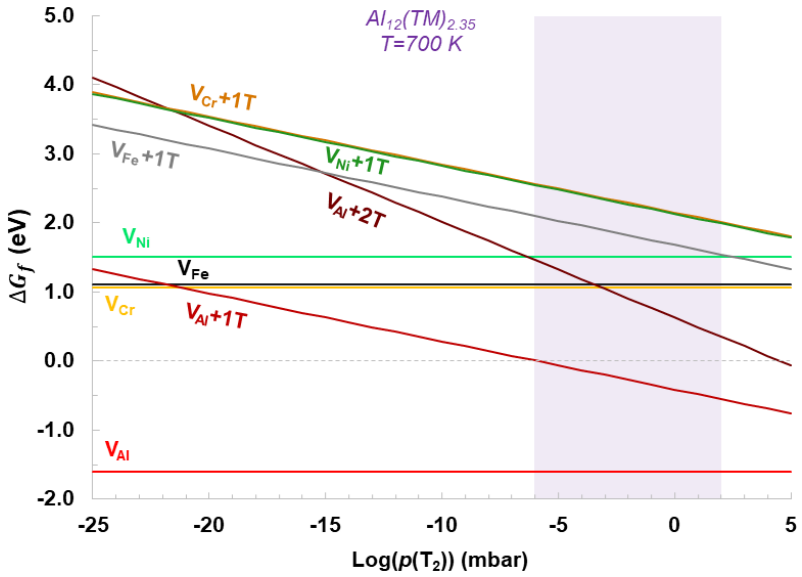

Figure 5: Gibbs free energy of non-tritiated and tritiated defects as function of tritium partial pressure ($p(T_2)$) at a temperature of 700 K. The purple area highlights the range of tritium partial pressure of interest.

3.5 Comparison of tritium trapping potential for various Fe-Al phases

By combining the theoretical results currently available informing about the thermodynamic of tritium in various Fe-Al coating phases, trends about tritium trapping can be drawn. A summary of the results is shown in Figure 6, in which Figure 6a reports the energy gain by trapping interstitial tritium into a metal vacancy. Positive energy values indicates that tritium remaining as an interstitial species is more favorable, while negative energies suggest that tritium prefers bind with a metal vacancy. A general trend is that tritium is favorably trapped by Al and Fe vacancies and preferentially forms Fe—T or Cr—T bonds, rather than Al—T or Ni—T bonds which are weaker, depending on the metal species surrounding the vacancy site. In the specific case of $Al_{12}(TM)_{2.35}$, tritium trapping by Al vacancies could still be favorable even if Figure 6a shows that the energy for tritium trapping is positive. In this material phase, the energy gained by creating an Al vacancy compensate the energetic cost of adding a tritium atom in it. While the series of

Fe-Al phases investigated do not have a lot of Ni or Cr species in their composition, trends regarding the trapping potential for these species are still elusive.

However, it is interesting to correlate the trapping trends of Figure 6a with the binding energy of interstitial tritium, shown in Figure 6b. In particular, it seems that when the binding energy of interstitial tritium is high, then trapping by a metal vacancy is preferred. For example, an interstitial tritium with a binding energy of less than 0.3 eV, as it is the case for $FeNiAl_5$ and $Al_{12}(TM)_{2.35}$, would not likely lead to a strong trapping by metal vacancies, as such, interstitial tritium would be the preferred chemical state. In contrast, if the binding energy of interstitial tritium is larger than 0.3 eV, as it is the case for Fe_4Al_{13} and the Fe_2Al_x series, then a trapping by metal vacancies is likely.

In Figure 6, the name of the Fe-Al phases that were observed by STEM in the outer-aluminide coating and inner-aluminide coating regions are written in red and green color respectively. While only one phase from the outer-aluminide coating region has been studied, it suggests that tritium could be trapped by different mechanisms. In the outer region, tritium would be trapped by Fe and Ni vacancies (and Al vacancies as long as ΔG_f is < 0), while in the inner region, tritium would be trapped by Al and Fe vacancies.

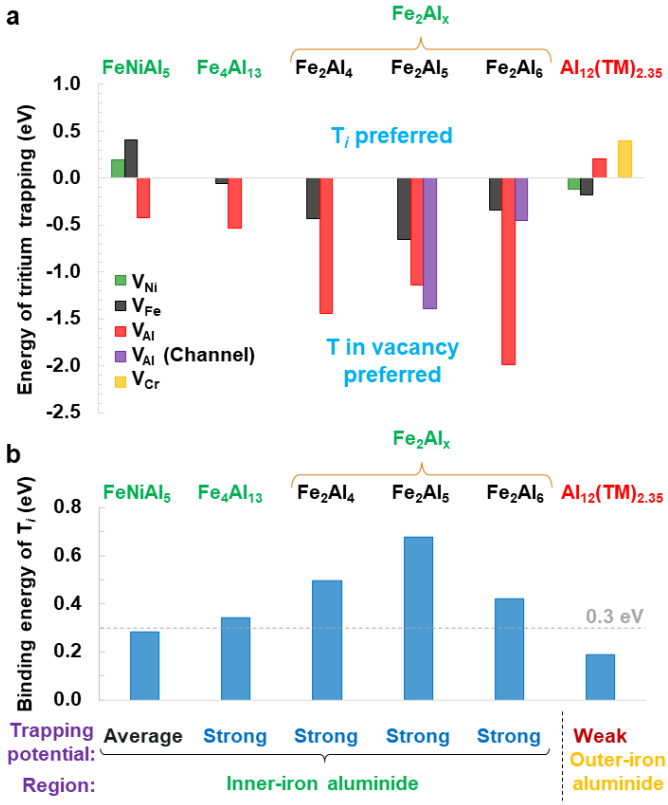

Figure 6: Comparison of tritium trapping potential for various Fe-Al phases. (a) Energy of trapping tritium in a metal vacancy. (b) Binding energy of interstitial tritium. Summary of the trapping potential of each Fe-Al phase and their location in the aluminide coating.

Conclusion

Density functional theory simulations have been carried out to investigate the potential for tritium trapping by metal vacancies in intermetallic $Al_{12}(TM)_{2.35}$ phase (TM = Fe, Cr, and Ni) as function of temperature and tritium partial pressure. It was found that tritium could be favorably trapped by Fe and Ni vacancies, and some Al vacancies, but not favorably trapped by Cr vacancies. While adding a tritium atom in an Al vacancy is not energetically favorable, the tritiated defect still has a negative Gibbs free energy because the energy gain for creating an Al vacancy compensate the energy cost of adding the tritium species. By combining the behavior of tritium in $Al_{12}(TM)_{2.35}$ and in previously studied Fe-Al coating phases (i.e., $FeNiAl_5$, Fe_4Al_{13}, and $Fe_2Al_{5.6}$), we found that there is a correlation between interstitial tritium binding energy and the potential for vacancy trapping. The current trend suggests that if the insertion of an interstitial tritium cost more than 0.3 eV, then trapping by metal vacancies should be preferred. By combining the simulations results obtained to date, we noticed different trapping mechanisms of tritium in the Al coating. In the outer-iron aluminide coating phase, $Al_{12}(TM)_{2.35}$, tritium is weakly trapped by Fe and Ni vacancies, and some Al vacancies, while in the inner-iron aluminide phases ($FeNiAl_5$, Fe_4Al_{13}, $Fe_2Al_{5.6}$) tritium should be more strongly trapped by Al and Fe vacancies. Altogether, these studies show that tritium interacts differently with the various Fe-Al aluminide phases found in the coating, however, they also suggest that tritium trapping and retention could be more efficient if metal defects are present and if the solubility of interstitial tritium in the different phases is low.

Acknowledgments

This research was supported by the National Nuclear Security Administration (NNSA) of the U.S. Department of Energy (DOE) through the Tritium Science Research Supporting the Tritium Modernization Program (TMP) managed by Pacific Northwest National Laboratory (PNNL). The authors thank the PNNL Institutional Computing (PIC) facility for providing computational resources.

4.0 References

1. Burgeson, I.E. “Watts Bar Cycle 12 Rod 2A PIE Protium and Tritium Assay Results”.
2. Sassi M., A.M. Chaka, D.J. Senor, and A.M. Casella. **2022**. “First-Principles Study of Tritium Trapping by Point Defects in Fe-Al Aluminide Coating Phases”. PNNL-33519. Richland, WA: Pacific Northwest National Laboratory.
3. Olszta, M. “Advanced Electron Microscopy for the TTP Program”. Presentation **(May 2022)**.
4. Jiang, W. *et al.* Carbonaceous deposits on aluminide coatings in tritium-producing assemblies. *Nuclear Materials and Energy* **25**, 100797 (2020).
5. Sassi M., D.J. Senor, and A.M. Casella. **2023**. “Ab Initio Simulations of Tritium Diffusion in Al_2O and Intermetallic $Al_{12}(TM)_{2.34}$ Aluminide Coating Phases”. PNNL-34818. Richland, WA: Pacific Northwest National Laboratory.
6. Kresse, G.; Furthmüller, J. Efficient iterative schemes for ab initio total-energy calculations using a plane-wave basis set. *Phys. Rev. B* **54**, 11169-11186 (1996).
7. Perdew, J.P.; Burke, K.; Ernzerhof, M. Generalized Gradient Approximation Made Simple. *Phys. Rev. Lett.* **77**, 3865-3868 (1996).
8. Monkhorst, H.J.; Pack, J.D. Special points for Brillouin-zone integrations. *Phys. Rev. B* **13**, 5188 (1976).
9. Togo, A. and Tanaka, I. First principles phonon calculations in materials science. *Scr. Mater.* **108**, 1-5 (2015).
10. Sui, H. X.; Liao, X. Z.; Kuo, K. H.; Zou, X.; Hovmöller, S. Structural Model of the Orthorhombic Non-Fibonacci Approximant in the $Al_{12}Fe_2Cr$ Alloy. *Acta Cryst.* **B53**, 587-595 (1997).
11. Luscher, W.G; Senor, D.J.; Clayton, K.K.; Longhurst, G.R. “In situ measurement of tritium permeation through stainless steel”. *J. Nucl. Mater.* **437**, 3730379 (2013).

Pacific Northwest National Laboratory

902 Battelle Boulevard
P.O. Box 999
Richland, WA 99354
1-888-375-PNNL (7665)

www.pnnl.gov